IEEE Journal of Translational Engineering in Health and Medicine

Received 22 June 2013; revised 15 October 2013; accepted 10 November 2013. Date of publication 19 November 2013; date of current version 10 December 2013.

Digital Object Identifier 10.1109/JTEHM.2013.2291555

Detection of Cardiac Quiescence from B-Mode Echocardiography Using a Correlation-Based Frame-to-Frame Deviation Measure

CARSON A. WICK[1] (Student Member, IEEE), JAMES H. MCCLELLAN[1] (Fellow, IEEE), LAKSHMINARAYAN RAVICHANDRAN[2] (Member, IEEE), AND SRINI TRIDANDAPANI[2] (Senior Member, IEEE)

[1]School of Electrical and Computer Engineering, Georgia Institute of Technology, Atlanta, GA 30332, USA
[2]Department of Radiology and Imaging Sciences, Emory University, Winship Cancer Institute, Atlanta, GA 30322, USA

CORRESPONDING AUTHOR: S. TRIDANDAPANI (stridan@emory.edu)

This work was supported by the PHS under Grant KL2 RF025009 from the Clinical and Translational Science Award Program, the National Institutes of Health, the National Center for Research Resources, and in part by Award Number K23EB013221 from the National Institute of Biomedical Imaging and Bioengineering. The work of J. H. McClellan was supported by the John and Marilu McCarty Chair.

ABSTRACT Two novel methods for detecting cardiac quiescent phases from B-mode echocardiography using a correlation-based frame-to-frame deviation measure were developed. Accurate knowledge of cardiac quiescence is crucial to the performance of many imaging modalities, including computed tomography coronary angiography (CTCA). Synchronous electrocardiography (ECG) and echocardiography data were obtained from 10 healthy human subjects (four male, six female, 23–45 years) and the interventricular septum (IVS) was observed using the apical four-chamber echocardiographic view. The velocity of the IVS was derived from active contour tracking and verified using tissue Doppler imaging echocardiography methods. In turn, the frame-to-frame deviation methods for identifying quiescence of the IVS were verified using active contour tracking. The timing of the diastolic quiescent phase was found to exhibit both inter- and intra-subject variability, suggesting that the current method of CTCA gating based on the ECG is suboptimal and that gating based on signals derived from cardiac motion are likely more accurate in predicting quiescence for cardiac imaging. Two robust and efficient methods for identifying cardiac quiescent phases from B-mode echocardiographic data were developed and verified. The methods presented in this paper will be used to develop new CTCA gating techniques and quantify the resulting potential improvement in CTCA image quality.

INDEX TERMS Coronary angiography, computed tomography, echocardiography, cardiac gating, electrocardiography.

I. INTRODUCTION

Accurate detection of cardiac quiescence is crucial for many cardiac imaging modalities including cardiac computed tomography (CT) and magnetic resonance imaging (MRI) [1]. To minimize motion artifacts and blurring in cardiac images, it is necessary to acquire image data during quiescent phases of the cardiac cycle, i.e., when the heart is quasi-stationary. Current methods for predicting quiescent phases, and in turn triggering image data acquisition, rely almost exclusively on the electrocardiogram (ECG). As an indirect representation of the mechanical state of the heart, ECG has been shown to be imprecise in predicting quiescent phases due to subject and heart-rate variability [2], [3]. It is therefore desirable to detect quiescence from a mechanically derived signal of cardiac activity. For this work, cardiac quiescence will be detected from B-mode echocardiographic cine data using two frame-to-frame deviation-based methods. Active contour feature tracking will be used to validate these methods.

The imaging performance of both cardiac CT and MRI relies heavily on cardiac gating. Accurate gating ensures that data acquisition occurs during periods of cardiac quiescence,

consequently minimizing blurring in the resulting CT images. In addition, accurate gating is necessary to ensure that the heart is in the same position in the image plane for techniques requiring data acquisition over multiple cardiac cycles. One application where accurate gating is crucial is CT coronary angiography (CTCA) [1]. CTCA is a promising alternative to the much more invasive catheter coronary angiography (CCA). More than 1.1 million CCAs are performed annually in the United States of America costing approximately $40 billion and resulting in more than 14,000 major complications [4]. Furthermore, nearly 40% of these tests reveal no coronary artery disease (as defined by less than 20% vessel stenosis) [5]. Conversely, CTCA does not require catheterization and is thus a less invasive and cost-effective alternative.

Echocardiography, i.e., ultrasound of the heart, will be used as the modality to investigate quiescence due to its real-time nature, high temporal resolution, accessibility, and lack of ionizing radiation. In particular, because echocardiography directly provides cardiac motion information, it allows for the accurate assessment of cardiac quiescence. B-mode echocardiographic data consists of a sequence of two-dimensional images, allowing for the application of image processing methods, and provides insight into the in-plane two-dimensional motion of the heart as a function of time. Echocardiographic tissue Doppler imaging (TDI) is often used for measuring the velocity of the myocardium in the direction of the ultrasound interrogation. TDI relies on the Doppler shift of the received ultrasonic pulses to calculate tissue velocity. While TDI is an efficient, straightforward measurement of cardiac motion, it is only sensitive in the direction of the pulse and therefore cannot capture the two-dimensional motion that can be derived from B-mode data. In order to better understand and more accurately predict quiescent phases, the interventricular septum (IVS) will be observed using active contour based tracking and frame-to-frame deviation measurement techniques. The IVS was chosen because it has been shown to be an accurate indicator of cardiac and, importantly for CTCA, coronary vessel quiescence [6].

The remainder of this paper is organized as follows. Section II starts with a description of the frame-to-frame deviation measures used to identify quiescent phases. Then, the active contour techniques used to perform feature segmentation and tracking are provided. In Section III, the quiescence detection methods are verified and compared using Bland-Altman analysis. For the 10 subjects examined, cardiac quiescence is presented graphically and numerically. Lastly, a discussion on the application of the methods and the implications of this work on cardiac imaging is given in Section IV.

II. Methods and Procedures

A. Subject Data Acquisition

For this work, ECG and echocardiographic data were synchronously acquired from 10 human subjects with no known cardiac conditions (4 male, 6 female, 23-45 years) using an Ultrasonix SonixTouch ultrasound machine (Analogic, Peabody, MA, USA). Emory University's Institutional Review Board approved the subject evaluations, and full, written, informed consent was obtained from each subject. The IVS was observed from the apical four-chamber view. For all but the first three subjects, data were recorded in multiple 10-second intervals during breath hold. The first two subject datasets consist of two 30-second intervals recorded pre- and post-exercise without breath hold. This choice was originally made to observe the effect of heart rate on cardiac quiescence. The third subject dataset was acquired during one breath hold. ECG data were acquired at a rate of 200 Hz while B-mode data were acquired at frame rates of either 30 or 50 frames per second (fps).

B. Frame-to-Frame Deviation Measurement Methods

The underlying cause of motion blur is movement during imaging data acquisition. If the heart is stationary for some period of a B-mode sequence, the image content of each frame during that period will be very similar. In this sense, frame-to-frame dissimilarity, *deviation*, can be associated with movement and hence consecutive frames with low deviation correspond to cardiac quiescence.

For this work, deviation between frames will be expressed as a negative function of the Pearson correlation coefficient taken over the IVS as it has been shown to be a strong indicator of image similarity [7]. Here, the Pearson correlation can be thought of as a measure of the similarity between two frames and is defined as

$$\rho\left(I_i, I_j\right) = \frac{\sum_{(x,y)\in I}\left(I_i\left(x,y\right)-\bar{I}_i\right)\left(I_j\left(x,y\right)-\bar{I}_j\right)}{\sqrt{\sum_{(x,y)\in I}\left(I_i\left(x,y\right)-\bar{I}_i\right)^2\sum_{(x,y)\in I}\left(I_j\left(x,y\right)-\bar{I}_j\right)^2}}, \quad (1)$$

where I_i is frame i, $\bar{I}_i$ is the mean of I_i, and (x, y) indexes each frame.

The correlation-based frame-to-frame deviation measure was calculated from a user-selected static rectangular region containing the IVS. For this work the region was selected by a graduate researcher and verified by a physician. This process could be automated if necessary [8]. The deviation calculation of the region of interest (ROI) is summarized as

$$\mathbf{D}\left(i,j\right) = 1-\rho(I_i, I_j) = 1-\frac{\sum_{(x,y)\in S}\left(I_i\left(x,y\right)-\bar{I}_i^S\right)\left(I_j\left(x,y\right)-\bar{I}_j^S\right)}{\sqrt{\sum_{(x,y)\in S}\left(I_i\left(x,y\right)-\bar{I}_i^S\right)^2\sum_{(x,y)\in S}\left(I_j\left(x,y\right)-\bar{I}_j^S\right)^2}}, \quad (2)$$

where I_i is frame i, S is the constant rectangular image region over which correlation is calculated, $\bar{I}_i^S$ is the mean of I_i in S, and x and y index image I_i and I_j. For this work, S is chosen so that the cardiac feature of interest is contained in S for all frames. This is accomplished by observing the beginning of the B-mode sequence for at least one cardiac cycle.

IEEE Journal of Translational Engineering in Health and Medicine

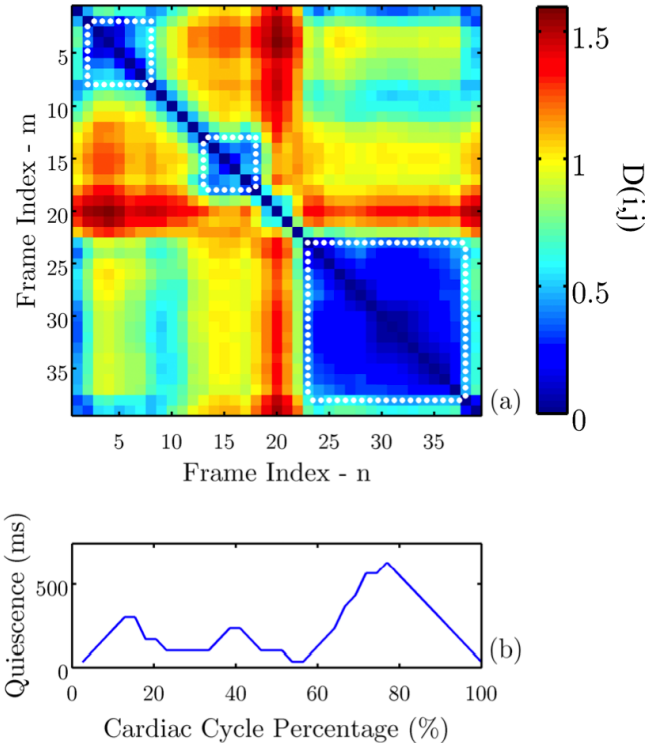

FIGURE 1. Graphical representation of quiescence detection from a deviation matrix, D (a), and the corresponding quiescence plot (b). One cardiac cycle is shown with a period of 1.2 seconds. Quiescent phases are indicated by dotted white squares where the mean value of D was chosen as the threshold.

Frame-to-frame deviation measurements for all possible comparisons of frame pairs for a given B-mode sequence are calculated according to (2) and recorded as a *deviation matrix*, $\mathbf{D}(i, j)$, where i and j are the time indices of the frames. When viewed as an image, this allows for the frame-to-frame deviation of the entire sequence to be efficiently observed, as shown in Fig. 1(a) for one cardiac cycle.

1) Quiescence from Deviation Measurements

Cardiac quiescence occurs when velocity is minimal. In turn, this corresponds to low deviation between neighboring frames in the cardiac sequence. As such, square regions of low deviation along the diagonal of the deviation matrix, $\mathbf{D}(i, j)$, indicate cardiac quiescent phases. The process of calculating the timing and duration of these phases was automated. For each point along the diagonal of $\mathbf{D}(i, j)$, the mean deviation measure of a square neighborhood centered at that point is calculated. The size of this neighborhood is increased until the mean deviation is no longer below a specified threshold, the mean of $\mathbf{D}$ in this case. Here the quiescence, $q(i)$, for each time instance, i, is defined as the duration of the gating window centered at i indicated by the width of the largest square region centered at $\mathbf{D}(i, i)$ with mean deviation below a specified threshold (Fig. 1(b)). This method can be seen as an extension of the one-dimensional, M-mode method presented in [2] to two-dimensional B-mode data.

2) Velocity from Deviation Measurements

The deviation measure, $\mathbf{D}(i, j)$, can be shown to be nearly linear with feature displacement assuming the feature is rigid and the motion linear between frames i and j, as described in the Appendix. Given a B-mode sampling period of 20 to 33 ms, these assumptions are reasonable for neighboring frames and $\mathbf{D}(i, i + 1)$ is a suitable approximation of the velocity magnitude of the IVS within a scaling factor and constant offset. If necessary, the approximation of the velocity from $\mathbf{D}$, defined as

$$v_{\mathbf{D}}(i) = \mathbf{D} \tag{3}$$

can be fit to a reference velocity provided by the active contour tracking methods described by (6). This process is summarized in the Appendix by (12-14). Alternatively, the approximated signals can be normalized and the velocity magnitude expressed in arbitrary units.

Interpolated velocity maps expressed in arbitrary units were calculated (see Fig. 2) to assist in the visual identification of cardiac quiescent phases. The velocity of each cardiac cycle, segmented by the R-peaks of the synchronously acquired ECG signal, is normalized to have a minimum of zero and a mean of one. This choice was made to eliminate the dependence on the maximum velocity, which was observed to vary more than the minimum and mean between cycles and acquisitions. Cubic interpolation was used to fit the data to a uniform grid, allowing velocity to be displayed as a function of heart rate and cardiac cycle phase. An example of the interpolated velocity map for Subject 4 is shown in Fig. 2, with the blue regions corresponding to minimal velocity and cardiac quiescence. From Fig. 2, the systolic and diastolic quiescent phases can be readily identified and the relative durations of these phases with respect to heart rate can be observed.

C. Active Contour Tracking

For this work, active contour tracking is used to validate the frame-to-frame deviation measures in regards to approximating the velocity magnitude of the IVS. Active contour methods provide a flexible framework for feature-based segmentation from image data. Active contour evolution relies both on constraints placed on the shape of the contour by the user and on the image characteristics along the contour. The balance of these two effects is tuned based on application and content of the image or sequence.

Classical active contour methods rely on discretizing the contour as a series of vertices, often referred to as *snaxels*, resulting in a contour $C(p) = \langle x(p), y(p) \rangle$ where p is the contour length parameterized and normalized to one [9]. The solution contour is found by minimizing the energy of the contour expressed as

$$E_{contour} = \int_0^1 \left(E_{int}\left(C\left(p\right)\right) + E_{img}\left(C\left(p\right)\right) \right) dp, \tag{4}$$

where E_{int} is the energy associated with the shape of the contour and E_{img} is the energy associated with the image content.

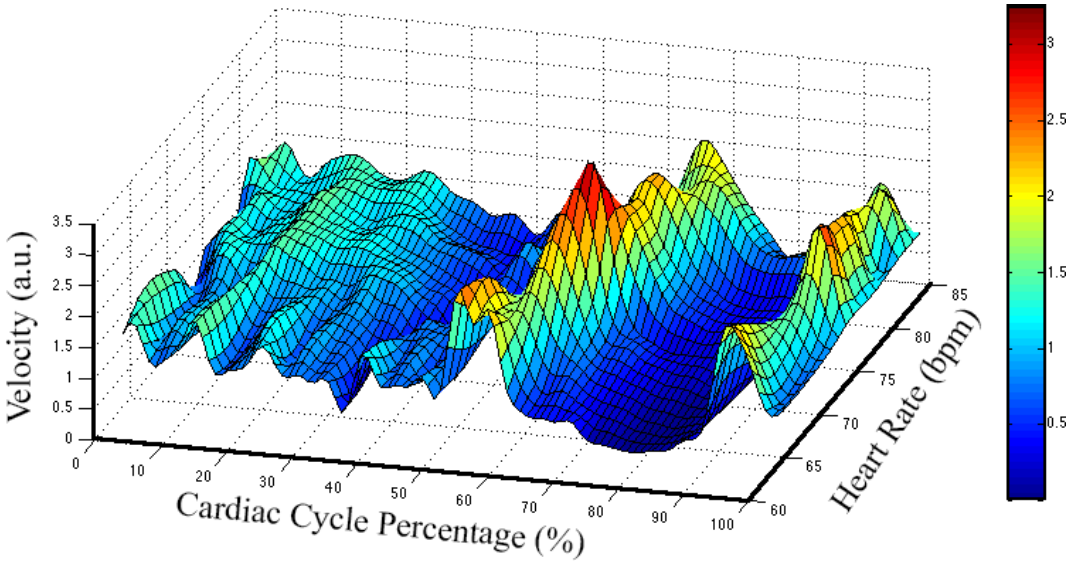

FIGURE 2. **Surface plot of the interpolated velocity from $v_D(i)$ for all cardiac cycles observed for Subject 4. Cardiac cycle percentage is shown on the x-axis, instantaneous heart rate on the y-axis, and velocity magnitude on the z-axis. Velocity is also represented by color according to the colorbar on the right. Note that, as expected, the diastolic quiescent phase centered at approximately 75% of the cardiac cycle decreases in duration as heart rate increases.**

E_{img} is most often chosen to be a decreasing function of the gradient of the image in order to attract the contour to edges in the image.

Extending active contour models to a sequence of frames is generally accomplished by finding the active contour on a frame-by-frame basis with each frame being solved with knowledge of only the current and previous frame. The solution of the previous frame is used as an estimate for the contour position in the following frame. Different schemes, such as optical flow [10] and Kalman filtering [8], are often employed to improve the estimation of the contour position in the next frame.

Active contours for this work are solved using a method based on [10], where optical flow is calculated according to [11] for the B-mode sequence and used in conjunction with the previous active contour solution to estimate the position of the contour in the subsequent frame. Optical flow attempts to estimate frame-to-frame movement by defining a small neighborhood around each pixel in the current frame and then locating this neighborhood in the following frame.

The cardiac-feature tracking algorithm identifies the feature of interest in each frame of B-mode data. The algorithm is initialized with the user providing an approximate outline consisting of 10 points along the boundary of the cardiac feature in the first frame of the sequence. The rough contour defined by these points is upsampled by five resulting in the evolution of a contour defined by 50 discrete points. The numerical active contour technique presented in [12] is used to find the outline of the feature in each frame by minimizing (4). For all frames after the first, the position of the previous contour, along with optical flow data of the sequence, is used to initialize the active contour algorithm.

1) Velocity from Active Contour Tracking

Knowledge of the velocity magnitude of the cardiac anatomic feature of interest can be used to validate the approximation provided by the frame-to-frame deviation methods. The velocity magnitude can be calculated from the two-dimensional velocity of the feature obtained by differencing the position of the contour in each frame. The position is calculated for each frame by finding the centroid of the cardiac feature, defined as the average location of the pixels inside the contour,

$$\bar{x}_i = \frac{1}{N}\sum_{x\in S_i} x, \quad \bar{y}_i = \frac{1}{N}\sum_{y\in S_i} y, \tag{5}$$

where S_i is the set of all pixel locations inside the contour $\mathbf{X}_i$ and N is the number of elements in S_i. The velocity magnitude of the feature can then be found by approximating the two-dimensional velocity obtained by taking the first difference of $\bar{x}_i$ and $\bar{y}_i$. This process is summarized by

$$v_{AC}(i) = \sqrt{(\bar{x}(i) - \bar{x}\,(i-1))^2 + (\bar{y}(i) - \bar{y}\,(i-1))^2}, \tag{6}$$

with periods of low velocity magnitude corresponding to phases of cardiac quiescence.

D. Experimental Setup

To assess the efficacy of B-mode detection of cardiac quiescence as well as the characteristics of cardiac quiescent phases for a small healthy population (10 subjects, 23-45 years old) the following results are provided. First, active contour tracking was validated in the direction of ultrasonic interrogation using synchronously acquired TDI data. Next, the velocity magnitude of the IVS from the deviation measure, $v_{\mathbf{D}}(i)$, was confirmed using active contour tracking.

IEEE Journal of Translational Engineering in Health and Medicine

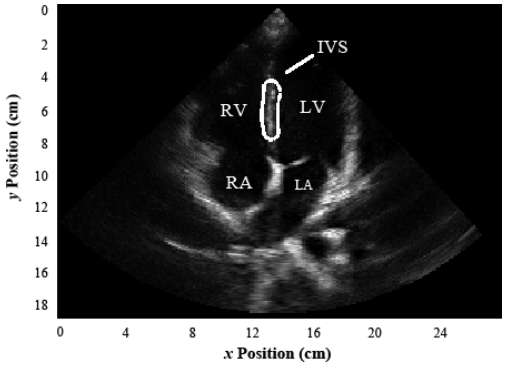

FIGURE 3. B-mode frame obtained from an apical four-chamber view of the heart, with solved contour shown around the IVS. The four chambers: right ventricle (RV), right atrium (RA), left ventricle (LV), and left atrium (LA) are shown.

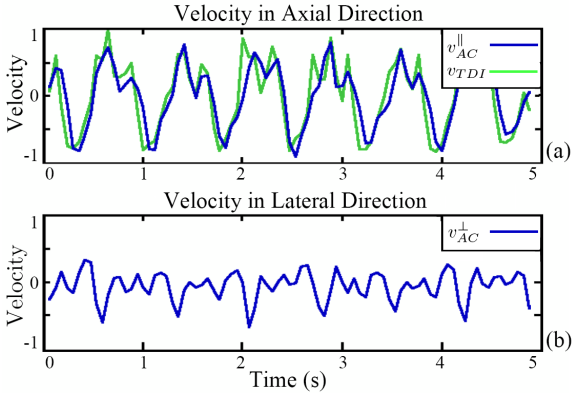

FIGURE 4. Velocity in the axial (a) and lateral (b) directions are shown with the active contour velocity, V_{AC}, and TDI velocity, V_{TDI}, in blue and green, respectively.

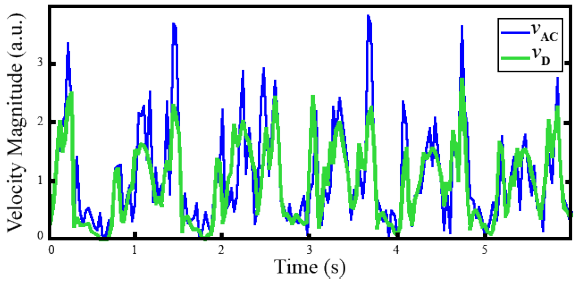

FIGURE 5. Comparison of active contour velocity, V_{AC}, and correlation based velocity, v_D, in blue and green, respectively. Note that the correlation based velocity approximation appears to have less noise in the quiescent phases with low velocity magnitude.

Then, Bland-Altman analysis was used to compare the quiescent phases indicated by the square regions of the deviation matrix, $\mathbf{D}(i, j)$, and the velocity, $v_{\mathbf{D}}(i)$. Lastly, the nature of the quiescent phases for the ten subjects was observed from $v_{\mathbf{D}}(i)$.

III. Results

A. Active Contour Tracking

The IVS was successfully segmented and tracked for seven of the 10 subjects using the active contour algorithm presented

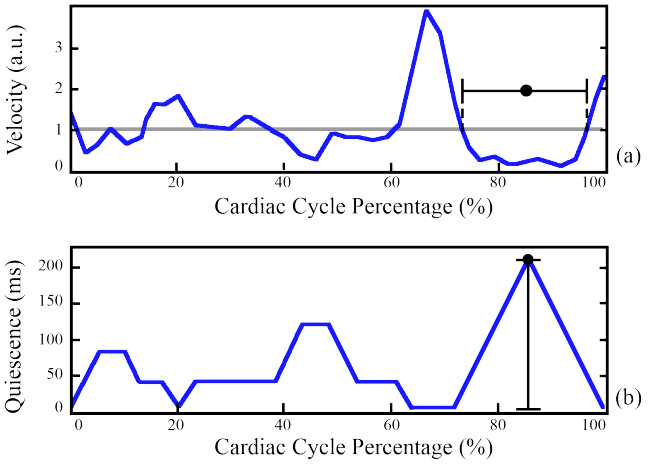

FIGURE 6. Comparison of diastolic quiescent phase identification methods for one cardiac cycle. Quiescent phases can be identified from both (a) the velocity signal, v_D, and (b) the quiescence, $q(i)$, from square regions of the deviation matrix.

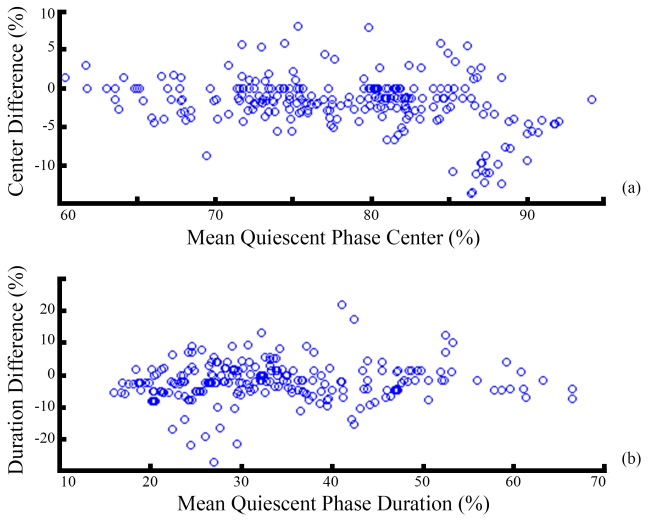

FIGURE 7. Comparison of diastolic quiescent phase identification methods for all cardiac cycles identified from both the velocity signal, v_D, and the square regions of the deviation matrix. The difference between the two measures is plotted on the vertical axis and the mean of the two measures is plotted on the horizontal axis. The cardiac cycle percentage of the phase centers (a) and durations (b) are plotted.

in Section II. For those not tracked, poor acoustic windows, acoustic shadowing, and out of plane motion proved problematic. Tracking was found to show little sensitivity to the initialization of the contour. An example of a solved active contour for a given frame is provided in Fig. 3. Here LV and RV are the left and right ventricle, and LA and RA are the left and right atrium. The position of the IVS was found for each frame using the centroid calculation given in (5). From the x- and y-position vectors, the velocity magnitude was calculated using first-difference methods as described in (6).

To verify the accuracy of the two-dimensional active contour tracking, the velocity calculated from the active contour centroids was compared to the velocity from synchronously

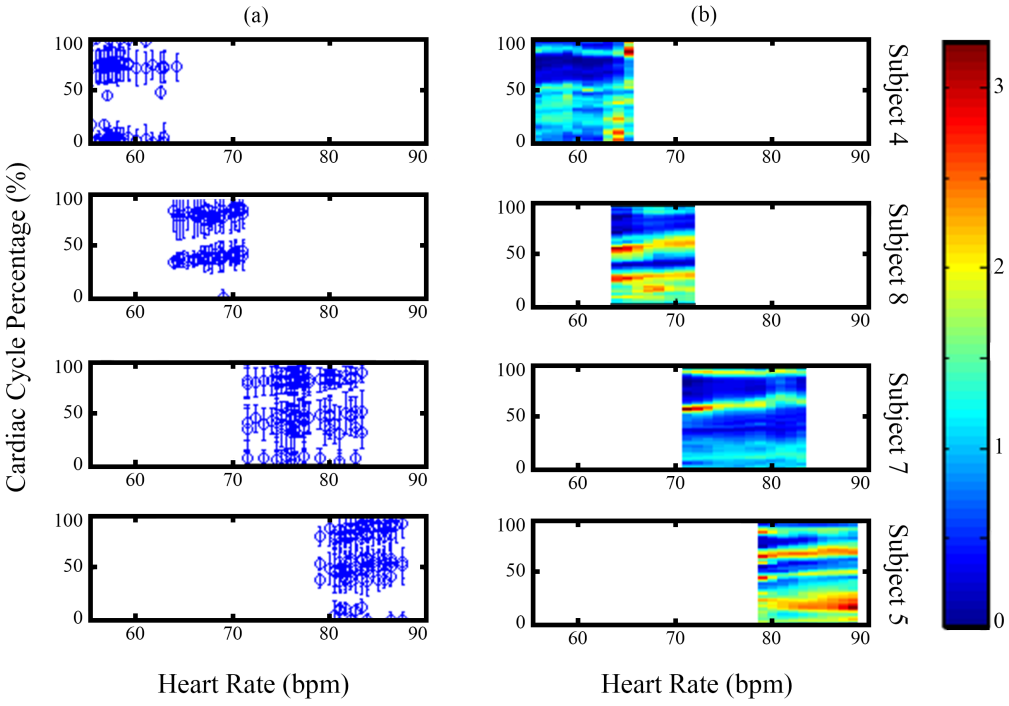

FIGURE 8. **Scatter plots (a) and velocity color maps (b) shown for four subjects. For the scatter plots the dots correspond to the quiescent phase centers and the bars correspond to the durations as determined using the velocity signal, v_D. For the color maps blue corresponds to low velocity magnitude and red corresponds to high velocity magnitude.**

acquired TDI data. As a direct measurement of tissue velocity based on the Doppler shift of the received ultrasonic pulses, TDI is often used to measure the one-dimensional velocity of cardiac features in the direction of ultrasonic interrogation. Active contour based velocity in the direction of ultrasonic interrogation, *axial direction*, was found to agree with that of TDI, indicating that active contours provide accurate velocity information. In addition, the active contour based velocity in the *lateral direction*, orthogonal to the direction of interrogation and not detected by TDI, was found to be significant. This suggests that B-mode derived two-dimensional velocity provides more complete IVS motion information than TDI. An example of these two normalized velocities is shown in Fig. 4. Clearly, the magnitude of the TDI velocity will be substantially different than the actual magnitude of the velocity, which is approximated by the velocity derived by active contours.

B. Quiescence from Frame-to-Frame Deviation

The deviation matrices, $\mathbf{D}(i, j)$, for each subject were calculated and the velocity of the IVS was approximated by the one-off diagonal of $\mathbf{D}(i, j)$, as described in Section II. Note that frame-to-frame deviation methods could be used for all 10 subjects as opposed to active contour methods that could only be used for seven subjects. To verify the accuracy of the velocity approximation, a number of velocity signals, $v_{\mathbf{D}}(i)$ from (3), were compared to the velocity signals derived from active contour tracking, $v_{AC}(i)$ from (6). Fig. 5 shows an example of this fitting and demonstrates that the velocity derived from the frame-to-frame deviation measure matches that derived from contour tracking. In addition, the velocity approximation based on correlation was observed to have less noise in the quiescent phases with low velocity magnitude. This is most likely due to noise that is accentuated by the differentiation of digital signals.

Quiescent phases were determined as regions of the velocity signal, $v_{\mathbf{D}}(i)$, less than the mean of $v_{\mathbf{D}}(i)$. Quiescence plots, $q(i)$, were then calculated by finding square regions along the diagonal of $\mathbf{D}(i, j)$ with average deviation under a specified threshold. The mean of $\mathbf{D}$ was used as the threshold for quiescence.

The center and duration of the diastolic quiescent phase for each cardiac cycle were then determined for the velocity and corresponding quiescence signals, $v_{\mathbf{D}}(i)$ and $q(i)$. For the quiescence signals the peak corresponding to the diastolic quiescent phase was found with the position and height indicating the center and duration of the quiescent phase, respectively. Both methods for identifying quiescent phases are depicted in Fig. 6

The center and duration of each diastolic quiescent phase detected from the velocity and quiescence signals were then compared for all subjects using Bland-Altman analysis to verify agreement between the measurement methods. As shown in Fig. 7, the two methods are nearly equivalent in determining quiescence.

IEEE Journal of Translational Engineering in Health and Medicine

TABLE 1. Summary of diastolic quiescent phase statistics.

	Quiescent Phase Center		Quiescent Phase Duration		Heart Rate		Cycles
	Mean	Std Dev	Mean	Std Dev	Mean	Std Dev	
Subject 1	74 %	6.4 %	451 ms	203 ms	60 bpm	10.7 bpm	61
Subject 2	70 %	4.4 %	352 ms	113 ms	58 bpm	5.7 bpm	39
Subject 3	75 %	4.3 %	203 ms	40 ms	99 bpm	5.9 bpm	10
Subject 4	74 %	1.4 %	324 ms	33 ms	58 bpm	2.3 bpm	37
Subject 5	79 %	6.6 %	246 ms	107 ms	63 bpm	1.5 bpm	31
Subject 6	86 %	4.8 %	188 ms	71 ms	83 bpm	2.1 bpm	43
Subject 7	82 %	2.2 %	182 ms	32 ms	77 bpm	2.8 bpm	42
Subject 8	84 %	3.4 %	301 ms	80 ms	68 bpm	2.0 bpm	39
Subject 9	75 %	2.4 %	446 ms	73 ms	59 bpm	2.3 bpm	35
Subject 10	72 %	8.1 %	150 ms	87 ms	66 bpm	2.9 bpm	23

Due to the similarity of the velocity and quiescence signals in determining quiescent phases, the velocity signal was chosen to display the analysis of the data due to computational efficiency, requiring only one correlation measure per time index. The nature of quiescent phases can be observed from Fig. 8 where the left column of plots indicates all quiescent phases observed longer than 83ms for four subjects and the right column of plots depicts the interpolated velocity maps of those subjects. The cutoff of 83ms was chosen as it corresponds to the minimum imaging time for a dual-source CT machine with a gantry rotation time of 333ms. As observed in practice, at high heart rates the systolic quiescent phase becomes proportionally longer than the diastolic phase [13], [14]. This is apparent for Subject 7 in Fig. 8(b) where the duration of the blue region in systole corresponding to minimal velocity becomes longer than that in diastole as heart rate increases.

The diastolic quiescent phase statistics for each of the 10 subjects are provided in Table I. Because the center and duration of the diastolic quiescent phase varies with heart rate, care should be taken in interpreting results for subjects who had a wide range in observed heart rates, indicated by a high heart rate standard deviation. From the table, a significant amount of inter- and intra-subject variability can be observed, suggesting that gating based solely on the ECG is suboptimal for predicting the timing of cardiac quiescent phases and that personalized gating protocols could improve this prediction.

IV. Conclusion

Two novel methods for determining cardiac quiescence from B-mode echocardiography were developed. These methods are based on frame-to-frame deviation measures of a user-specified image region and were verified using active contour tracking. The two-dimensional velocity derived from active contour tracking was validated in the axial direction using TDI. In addition, the lateral velocity component, not detected by TDI, was shown to be significant. This suggests that two-dimensional, image-based methods may prove more accurate in determining cardiac quiescence than the more straightforward TDI method of determining myocardial velocity.

These two methods for determining cardiac quiescence were used to analyze data for 10 subjects with no known cardiac conditions. The first method exploits the fact that the correlation between two frames is linearly related to feature displacement, given an assumption of linear motion and feature rigidity between the frames in question as described in the Appendix. The velocity calculated using the deviation of neighboring frames and verified using active contour tracking suggests that, at least for the IVS, these assumptions are reasonable. The second method for determining quiescence from the deviation attempts to identify quiescent phases as square regions of low deviation from the deviation matrix, $\mathbf{D}(i, j)$. Despite using more deviation measures to determine quiescence for each time index, it was observed that this method was actually more susceptible to noise. One possible explanation for this is that the deviation measures of a long sequence of frames allow more time for inadvertent transducer, subject, or breathing motion whereas with the velocity approximation technique, only neighboring frames are compared. Despite this, the two methods were found to agree with one another. The proposed deviation-based methods were able to identify quiescent phases for the three subjects where active contour tracking was not possible due to loss of tracking. It is important to note that although quiescent phases can be identified for B-mode sequences with poor imaging, accuracy may be decreased and cannot be verified by active contour tracking. In addition to robustness, these methods provide a less noisy velocity signal than that provided by active contour methods, as active contour tracking requires differentiation to obtain the velocity. Lastly, these methods are also much more computationally efficient than the active contour methods, requiring only correlation measures instead of solving complicated minimization problems and performing optical flow calculations for each B-mode frame. Although not required for the applications in this work, deviation-based velocity calculation could be done in real-time.

The choice of a region-based correlation method was made to provide a robust and efficient technique to determine the magnitude of the velocity of a specified ROI. Speckle tracking is another commonly used method to ascertain motion using optical flow to calculate the frame-to-frame displacement of the pixels inside an ROI [15]. For the application presented in this work, the pixel displacements could be averaged over the ROI to obtain the velocity magnitude of the cardiac feature in the ROI. This could then be used to find quiescent phases. Because pixel-level 2-D motion between frames is estimated, more descriptive motion quantification could be performed. However, speckle tracking is not without drawbacks. It requires high image quality and high B-mode frame rate (60-110 fps), placing substantial constraints on the imaging hardware. To minimize the effect of random noise, speckle tracking is usually averaged over at least three cardiac cycles, making speckle tracking for subjects with arrhythmias problematic. Lastly, speckle tracking is computationally expensive and as a result is generally performed offline after an examination.

Another recent technique for robustly quantifying motion leverages the fact that a translation of an object in the image plane corresponds to a phase shift in the Fourier domain [16]. By taking the 2-D Fourier transform of a sequence of images the 2-D velocity of the feature can be obtained from the phase shifts. Because this method relies on the Fourier transform and peak detection, it is more computationally expensive than the proposed region-based correlation method.

One potential concern with determining quiescence from the frame-to-frame deviation is that only the relative velocity magnitude is provided. Normalization of the velocity signals partially alleviates this concern because a constant threshold for quiescence can be employed. If needed, absolute velocity magnitude can be obtained either by fitting the deviation-based velocity to a reference velocity, e.g., the velocity from the active contour tracking, as described by (14-16), or by leveraging the relationship in (10). The latter method does not require a reference velocity and would rely on how well the relationship between the area of feature overlap between frames and the feature displacement is known.

Another potential limitation is that the subject population for this work is not necessarily representative of that expected to receive CTCA studies. However, the performance of echocardiography should be independent of subject population because echocardiography is not known to be limited by the age or cardiac health of the patient. Therefore, the proposed detection methods should be applicable for patients receiving CTCA studies.

Though Liu *et al.* showed that the IVS is a strong indicator of quiescence of the left anterior descending coronary artery [6], other arteries may have different quiescent phases. For low heart rates the optimal CTCA imaging window (and consequently the longest quiescent phase) occurs during the same cardiac phase during diastole for each coronary vessel. For higher heart rates, above 80 bpm, the longest quiescent phase occurs during systole and was shown to vary by 10% depending on the coronary artery in question, while the diastolic quiescent phases were the same [17]. This suggests that for high heart rates the longest quiescent phases determined by observing the IVS may not correspond exactly to those of some coronary vessels. Although this may be the case, the relationship between the quiescent phases of the IVS and those of the vessel in question may be deterministic, allowing for the actual quiescent phase to be obtained from that of the IVS. This is a topic for future investigation.

In light of these results, it is reasonable to suggest that the correlation of neighboring frames can be used to efficiently approximate the magnitude of the velocity of cardiac features, and hence cardiac quiescence. The applicability of this technique to other cardiac features is a topic for further research. In addition, the frame-to-frame deviation of multiple static regions corresponding to different cardiac features in the imaging plane could be used to analyze the relationship between the timing of the quiescent phases of the cardiac features in question.

From Table I, a significant amount of both inter- and intra-subject variability was observed as evidenced by the different means of the quiescent phase centers and significant standard deviations of those centers for each subject. This suggests that gating based on the mechanics of the heart rather than the ECG may provide better prediction of cardiac quiescent phases for the gating of CTCA and other cardiac imaging modalities. The quiescence detection methods presented here will be used for further study into such gating methods.

This work shows that the TDI misses a significant amount of velocity in the lateral direction. Therefore, it is likely that 2-D B-mode echocardiography motion estimation misses some amount of out-of-plane motion. Given 3-D echocardiographic data, the extension of the proposed deviation measures to 3-D is straightforward and a topic for future study.

This work addresses the first half of the gating problem, i.e., quiescence detection. However, the second half of the problem, quiescence prediction, while relying on accurate detection, is more complicated. By knowing the precise timing of cardiac quiescent phases, effective methods for quiescence prediction can be developed and analyzed. The phases detected using the methods proposed in this work can serve as a baseline to compare phases predicted using CT compatible techniques. Two potential techniques for cardiac-motion-informed gating are offline and real-time methods. Offline methods would focus on obtaining patient specific gating parameters prior to CTCA for the standard ECG gating that is currently in use. In this case, the proposed detection methods could be used directly. The amount of potential improvement in images using this approach is a topic for further study. Real-time gating involves predicting quiescent phases during the CTCA exam. As such, it is necessary for the sensing device used for gating to be CT compatible. Unfortunately, standard echocardiographic transducers are not CT compatible because of the extensive streak artifacts that they would cause in the CT images.

IEEE Journal of Translational Engineering in Health and Medicine

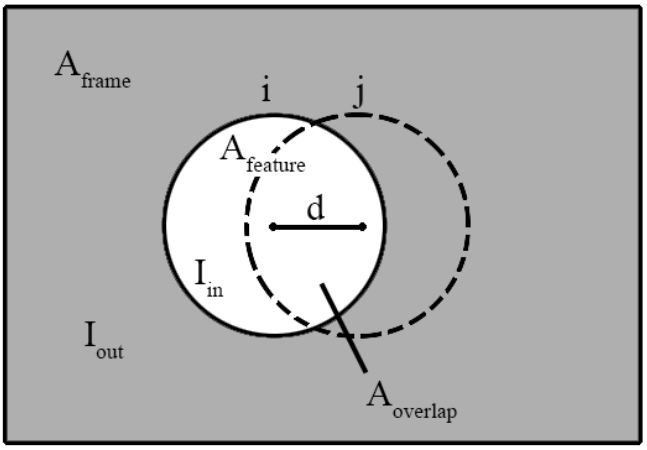

FIGURE 9. Definition of terms used in the theoretical example relating frame-to-frame deviation measures to feature velocity. The solid outline indicates the feature in frame *i* and the dashed outline indicates the feature in frame *j*, where the feature is displaced a distance of *d*.

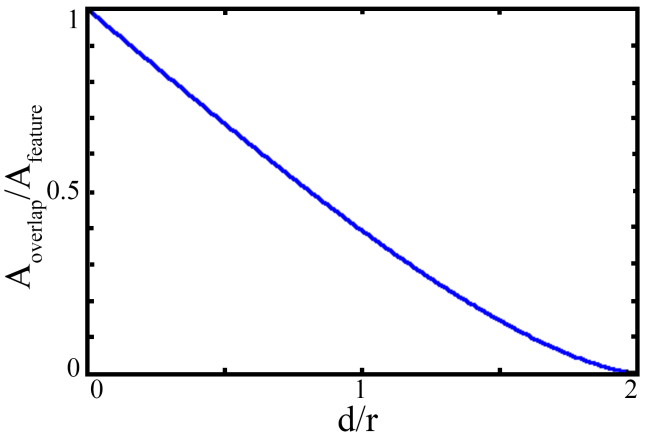

FIGURE 10. Normalized area of overlap, $A_{overlap}$, for a circle as a function of the ratio of the displacement, *d*, to the feature radius, *r*. When $d \geq 2r$ the overlapping area will be zero. For small displacement ($d/r < 1$), the function is very nearly linear.

Fortunately, two potential modalities have been shown to be CT compatible: TDI and seismocardiography (SCG) [18], [19]. There exist TDI specific transducers that are radiolucent and would not interfere with CT data acquisition. Though TDI was shown in this work to be insensitive to a significant amount of two-dimensional velocity, the performance of TDI in predicting quiescent phases was not investigated. SCG uses an accelerometer to measure the acceleration of the chest wall due to cardiac motion. Modern accelerometers are small enough to not interfere with CT acquisition and as such SCG could provide a cardiac-motion-based signal that could be used for predicting cardiac quiescent phases and gating CTCA [20]. For both TDI and SCG methods of real-time prediction, the methods proposed in this work could be used to assess the predictive accuracy of these methods.

In addition to being a direct indication of cardiac motion, signals derived from the mechanics of the heart would improve the quiescence predictive performance for patients with cardiac arrhythmias. This is true because the signal features that can be used for triggering are much nearer to the actual quiescent phase. This minimizes the effect of inaccurate cardiac cycle length prediction caused by arrhythmias. From initial investigations there exist detectable features of the SCG that are within 10% of the start of quiescence in terms of cardiac cycle phase. Contrasting this against the 70% from the R-peak of the ECG to the diastolic quiescent phase or 40% for the systolic quiescent phase, it is apparent that the predictive performance of mechanical based gating signals would be better than that of the ECG in the presence of cardiac arrhythmias.

Appendix

To better understand the relationship between the frame-to-frame deviation measure and cardiac feature velocity, it is useful to look at a simple theoretical example. Consider two frames, *i* and *j*, containing a cardiac feature of interest moving a distance *d*. Assume the feature is rigid and moves linearly between frames. Lastly, let the image intensities inside the contour, I_{in}, and outside the contour, I_{out}, be constant and let A_{frame} be the area of the frame over which correlation is to be calculated, $A_{feature}$ be the area of the feature of interest, and $A_{overlap}$ be the area of feature overlap between frames. These definitions are shown graphically in Fig. 9.

Given the assumptions above, it can be shown that for the correlation-based deviation measure in (2) that

$$\mathbf{D}(i,j) = 1 - \frac{A_{overlap}A_{frame} - A_{feature}^2}{A_{feature}A_{frame} - A_{feature}^2}, \tag{7}$$

where $\mathbf{D}(i,j)$ is the frame-to-frame deviation measure for a static correlation region between frames *i* and *j*. Because A_{frame} and $A_{feature}$ are constant, $\mathbf{D}(i,j)$ is only a function of $A_{overlap}$, which depends on the geometry and displacement of the feature. Also of note, is that this measure is independent of scale.

If the feature is circular, $A_{overlap}$ will be independent of the direction of the displacement and can be expressed as twice the area of the appropriate circular segment as shown below.

$$A_{segment}(d) = r^2 \cos^{-1}\left(\frac{d/2}{r}\right) - \frac{d}{2}\sqrt{r^2 - \left(\frac{d}{2}\right)^2}, \tag{8}$$

$$A_{overlap}(d) = 2 \cdot A_{segment}(d), \tag{9}$$

$$A_{overlap}(d) = 2r^2 \cos^{-1}\left(\frac{d}{2r}\right) - \frac{d}{2}\sqrt{4r^2 - d^2}, \tag{10}$$

where *d* is the feature displacement between the frames and *r* is the radius of the circle. Assuming linear motion between two consecutive frames *i* and *j*, the displacement *d* is related to feature velocity by

$$v = d \cdot f_{FR} \cdot (j - i), \tag{11}$$

where *v* is the magnitude of the feature velocity and f_{FR} is frame rate. $A_{overlap}$ for a circle (8) is shown in Fig. 10 as a function of the ratio of the displacement to the radius, d/r. Fig. 10 shows that for small *d* relative to *r*, $A_{overlap}$ is

very nearly linear. Because velocity, v, is linearly related to displacement, d, this results in a linear relationship between feature velocity and the correlation-based deviation measure, $\mathbf{D}(i, j)$.

Given the linearity of displacement, and subsequently velocity, with each deviation matrix, the following relation holds,

$$v(i) \propto \mathbf{D}(i, j) \cdot f_{FR} \cdot (j - i). \tag{12}$$

Assuming the motion is near linear during one sampling period, the velocity can be approximated by

$$v_{\mathbf{D}}(i) = \mathbf{D}(i, i + 1). \tag{13}$$

The true velocity can then be expressed as a linear function of $v_{\mathbf{D}}$,

$$v(i) = \alpha v_{\mathbf{D}}(i) + \beta, \tag{14}$$

where α and β are fitting constants. If provided a reference velocity, $v_{REF}(i)$, α and β can be expressed in a least squares sense as

$$\alpha = \frac{(v_{\mathbf{D}} - \bar{v}_{\mathbf{D}})^T (v_{REF} - \bar{v}_{REF})}{(v_{\mathbf{D}} - \bar{v}_{\mathbf{D}})^T (v_{\mathbf{D}} - \bar{v}_{\mathbf{D}})} = \frac{\mathrm{Cov}(v_{\mathbf{D}}, v_{REF})}{\mathrm{Var}(v_{\mathbf{D}})}, \tag{15}$$

$$\beta = \bar{v}_{REF} - \alpha \bar{v}_{\mathbf{D}}, \tag{16}$$

where $\bar{v}_{\mathbf{D}}$ and $\bar{v}_{REF}$ are the means of $v_{\mathbf{D}}$ and v_{REF}, respectively.

REFERENCES

[1] B. Desjardins and E. A. Kazerooni, "ECG-gated cardiac CT," *Amer. J. Roentgenol.*, vol. 182, no. 4, pp. 993–1010, Apr. 2004.

[2] S. Tridandapani, J. B. Fowlkes, and J. M. Rubin, "Echocardiography-based selection of quiescent heart phases," *J. Ultrasound Med.*, vol. 24, no. 11, pp. 1519–1526, Nov. 2005.

[3] K. R. Johnson, S. J. Patel, A. Whigham, A. Hakim, R. I. Pettigrew, and J. N. Oshinski, "Three-dimensional, time-resolved motion of the coronary arteries," *J. Cardiovascular Magn. Reson.*, vol. 6, no. 3, pp. 663–673, 2004.

[4] V. L. Roger, A. S. Go, D. M. Lloyd-Jones, E. J. Benjamin, J. D. Berry, W. B. Borden, *et al.*, "Heart disease and stroke statistics–2012 update: A report from the American heart association," *Circulation*, vol. 125, no. 1, pp. e2–e220, Jan. 2012.

[5] M. R. Patel, E. D. Peterson, D. Dai, J. M. Brennan, R. F. Redberg, H. V. Anderson, *et al.*, "Low diagnostic yield of elective coronary angiography," *New England J. Med.*, vol. 362, no. 10, pp. 886–895, Mar. 2010.

[6] G. Liu, X.-L. Qi, N. Robert, A. J. Dick, and G. A. Wright, "Ultrasound-guided identification of cardiac imaging windows," *Med. Phys.*, vol. 39, no. 6, pp. 3009–3018, Jun. 2012.

[7] M. Svedlow, C. D. McGillem, and P. E. Anuta, "Image registration: Similarity measure and preprocessing method comparisons," *IEEE Trans. Aerospace Electron. Syst.*, vol. AES-14, no. 1, pp. 141–150, Jan. 1978.

[8] J. A. Noble and D. Boukerroui, "Ultrasound image segmentation: A survey," *IEEE Trans. Med. Imaging*, vol. 25, no. 8, pp. 987–1010, Aug. 2006.

[9] M. Kass, A. Witkin, and D. Terzopoulos, "Snakes: Active contour models," *Int. J. Comput. Vis.*, vol. 1, no. 4, pp. 321–331, Jan. 1988.

[10] I. Mikic, S. Krucinski, and J. D. Thomas, "Segmentation and tracking in echocardiographic sequences: Active contours guided by optical flow estimates," *IEEE Trans. Med. Imaging*, vol. 17, no. 2, pp. 274–284, Apr. 1998.

[11] A. Singh, *Optic Flow Computation: A Unfied Perspective*. Piscataway, NJ, USA: IEEE Press, 1991.

[12] F. Leymarie and M. D. Levine, "Tracking deformable objects in the plane using an active contour model," *IEEE Trans. Pattern Anal. Mach. Intell.*, vol. 15, no. 6, pp. 617–613, Jun. 1993.

[13] H. Seifarth, S. Wienbeck, M. Püsken, K.-U. Juergens, D. Maintz, C. Vahlhaus, *et al.*, "Optimal systolic and diastolic reconstruction windows for coronary CT angiography using dual-source CT," *Amer. J. Roentgenol.*, vol. 189, no. 6, pp. 1317–1323, Dec. 2007.

[14] A. C. Weustink, N. R. Mollet, F. Pugliese, W. B. Meijboom, K. Nieman, M. H. Heijenbrok-Kal, *et al.*, "Optimal electrocardiographic pulsing windows and heart rate: Effect on image quality and radiation exposure at dual-source coronary CT angiography," *Radiology*, vol. 248, no. 3, pp. 792–798, Sep. 2008.

[15] S. Mondillo, M. Galderisi, D. Mele, M. Cameli, V. S. Lomoriello, V. Zacà, *et al.*, "Speckle-tracking echocardiography: A new technique for assessing myocardial function," *J. Ultrasound Med.*, vol. 30, no. 1, pp. 71–83, Jan. 2011.

[16] H. Sundar, A. Khamene, L. Yatziv, and C. Xu, "Automatic image-based cardiac and respiratory cycle synchronization and gating of image sequences," in *MICCAI*, vol. 5762. New York, NY, USA: Springer-Verlag, 2009, pp. 381–388.

[17] M. B. Srichai, E. M. Hecht, D. Kim, J. Babb, J. Bod, J. Bodd, *et al.*, "Dual-source computed tomography angiography image quality in patients with fast heart rates," *J. Cardiovascular Comput. Tomogr.*, vol. 3, no. 5, pp. 300–309, Sep. 2009.

[18] A. D. Waggoner and S. M. Bierig, "Tissue Doppler imaging: A useful echocardiographic method for the cardiac sonographer to assess systolic and diastolic ventricular function," *J. Amer. Soc. Echocardiogr.*, vol. 14, no. 12, pp. 1143–1152, Dec. 2001.

[19] J. M. Zanetti and D. M. Salerno, "Seismocardiography: A technique for recording precordial acceleration," in *Proc. 4th Annu. IEEE Symp. Comput., Based Med. Syst.*, May 1991, pp. 4–9.

[20] C. A. Wick, J. J. Su, J. H. McClellan, O. Brand, P. T. Bhatti, A. L. Buice, *et al.*, "A system for seismocardiography-based identification of quiescent heart phases: Implications for cardiac imaging," *IEEE Trans. Inf. Technol. Biomed.*, vol. 16, no. 5, pp. 869–877, Sep. 2012.

CARSON A. WICK (S'10) received the B.S. and M.S. degrees in electrical engineering from the Georgia Institute of Technology, in 2006 and 2007, respectively, where he is currently pursuing the Ph.D. degree. In 2008 and 2009, he was a Ph.D. Student Intern with the Digitally Enhanced Analog Systems Group, Texas Instruments DSP Research and Development Center, Dallas, TX, USA.

His current research is focused on digital signal processing of cardiac signals, with applications for motion analysis and tracking. He currently balances his research efforts between the Center for Signal and Information Processing at Georgia Tech and the Department of Radiology and Imaging Sciences, Emory University School of Medicine. He is a member of Eta Kappa Nu.

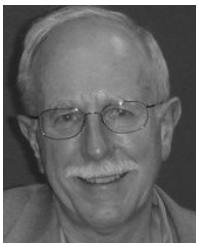

JAMES H. MCCLELLAN (S'69–M'74–SM'79–F'85) received the B.S. degree in electrical engineering from Louisiana State University in 1969, and the M.S. and Ph.D. degrees from Rice University in 1972 and 1973, respectively. From 1973 to 1982, he was a member of the research staff with the Lincoln Laboratory and a Professor at MIT. From 1982 to 1987, he was with Schlumberger Well Services. Since 1987, he has been a Professor with the School of Electrical and Computer Engineering, Georgia Tech, where he is currently the John and Marilu McCarty Chair.

He is the co-author of the texts *Number Theory in Digital Signal Processing, Computer Exercises for Signal Processing, DSP First: A Multimedia Approach*, and *Signal Processing First*, which received the McGraw-Hill Jacob Millman Award for an outstanding innovative textbook in 2003. In 1998, he received the W. Howard Ector Outstanding Teacher Award at Georgia Tech, and the Education Award from the IEEE Signal Processing Society in 2001. In 1987, he received the Technical Achievement Award for work on FIR filter design, and the Society Award both from the IEEE Signal Processing Society in 1996. In 2004, he was a co-recipient of the IEEE Jack S. Kilby Signal Processing Medal. He is a member of Tau Beta Pi and Eta Kappa Nu.

IEEE Journal of Translational Engineering in Health and Medicine

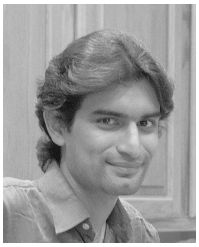

LAKSHMINARAYAN RAVICHANDRAN (S'08–M'11) received the B.E. degree in electronics and communication engineering from Visvesvaraya Technological University, Karnataka, India, in 2005, and the M.S. and Ph.D. degrees in electrical engineering from Arizona State University, Tempe, in 2008 and 2011, respectively. He was a Post-Doctoral Fellow in the Department of Radiology and Imaging Sciences, Emory University, Atlanta, from 2011 to 2012. He is currently with Mathworks, Inc., Bengaluru, India.

His primary research interests are in the areas of development of signal and image processing algorithms, analysis of biomedical data, and architectural implementation of signal processing algorithms. He received the Teaching Excellence Award from the Graduate and Professional Student Association at Arizona State University in 2011.

SRINI TRIDANDAPANI (S'86–M'95–SM'12) received the B.E. degree from Anna University, Madras, India, and the M.S.E.E. and Ph.D. degrees from the University of Washington, Seattle, all in electrical engineering. After post-doctoral training in computer science at the University of California, Davis, CA, USA, he was an Assistant Professor of electrical and computer engineering with Iowa State University, Ames, IA, USA. He received the M.D. degree from the University of Michigan, Ann Arbor, MI, USA, followed by residency training in radiology at Michigan. He received clinical fellowships in cardiothoracic imaging and abdominal imaging with Emory University. He received the master's degree in clinical and translational research from Emory University.

A board-certified radiologist, he is currently a faculty member of the Department of Radiology and Imaging Sciences, Emory University, and an Adjunct Professor with the School of Electrical and Computer Engineering, Georgia Institute of Technology. His current research involves the development of novel gating strategies for optimizing cardiac computed tomography and innovative tools to increase patient safety in medical imaging.